

# Direct sampling of complex landscapes at low temperatures: the three-dimensional $\pm J$ Ising spin glass

Alexander K. Hartmann\*

*Institut für Theoretische Physik, University of Göttingen, Bunsenstr. 9, 37073 Göttingen, Germany*

Federico Ricci-Tersenghi†

*Dipartimento di Fisica and INFM, Università di Roma “La Sapienza”, Piazzale Aldo Moro 2, I-00185 Roma (Italy)*

(Dated: December 2, 2024)

A method is presented, which allows to sample directly low-temperature configurations of glassy systems, like spin glasses. The basic idea is to generate ground states and low lying excited configurations using a heuristic algorithm. Then, with the help of microcanonical Monte Carlo simulations, more configurations are found, clusters of configurations are determined and entropies evaluated. Finally equilibrium configuration are randomly sampled with proper Gibbs-Boltzmann weights.

The method is applied to three-dimensional Ising spin glasses with  $\pm J$  interactions and temperatures  $T \leq 0.5$ . The low-temperature behavior of this model is characterized by evaluating different overlap quantities, exhibiting a complex low-energy landscape for  $T > 0$ , while the  $T = 0$  behavior appears to be less complex.

PACS numbers: PACS Numbers: 75.10.Nr, 75.50.Lk, 75.40.Mg, 05.50.+q

## I. INTRODUCTION

Despite large efforts made by the scientists in the last two decades, complex energy landscapes with many local minima and nested valleys, like that of spin glasses<sup>1</sup>, still offer many relevant questions to be answered. These questions usually regard the lowest energy levels of the landscape. The traditional numerical approach is to apply a Monte Carlo (MC) simulation<sup>2</sup>. Equilibration is tested by monitoring different average quantities as a function of the number of MC steps. Equilibration can be assumed, when the measured values of different runs, initially being far apart, agree within error bars. Another approach<sup>3</sup> is to calculate one quantity, like the link overlap, in two different ways, one time directly and one time depending on some other measured quantity like the energy, and wait till both results agree.

Such a test is available only in special cases, e.g. for spin glasses with a Gaussian distribution of the bonds. Otherwise, one usually waits till the quantity of interest does not show any more a time dependence. Nevertheless, at low temperatures and with increasing system size, equilibration becomes much harder and eventually, at very low temperatures, is impossible.

In the very last years, a different approach has been proposed, namely the calculation of ground-state (GS) and low-energy configurations. Some characteristics of the low-energy landscape can be probed by the application of suitable perturbations which slightly modify the GS<sup>4</sup>. But the full information on the low-temperature behavior can be obtained only by an equilibrium sampling of the system at a given temperature. Here we show, that by calculating GS and excited states, one can directly sample very low temperatures. Several algorithms and heuristics<sup>5</sup> are available to obtain ground states and excited states. Some are based again on Monte Carlo techniques like simulated annealing (SimA) and parallel

tempering (PT). All these techniques have the drawback, that it is impossible to obtain an unbiased, i.e. equilibrium sample of configurations for  $T \rightarrow 0$ . For the MC methods, the reason is that for larger systems and very low temperatures, equilibration times are too long. We shall give below an example which shows for a  $\pm J$  Ising spin glass, which exhibits an exponential ground state degeneracy, that just obtaining ground states is much easier than obtaining ground states with their proper statistics, i.e. each ground state with the same probability. For other existing heuristics the statistics of the configurations is influenced in an uncontrollable way by the low-energy landscape.

In this work, a post-processing method is presented, which removes the bias induced by the non-equilibrium low-temperature sampling and allows to obtain a properly equilibrated state for systems having a high degeneracy. The basic idea of the technique is to calculate clusters of configurations, which are connected in configuration space by zero-energy moves, e.g. zero-energy flips of spins in the Ising spin-glass case. Next, the sizes of these clusters are estimated and used to obtain an unbiased sample, where each cluster contributes with a factor to the size of the cluster and to the Gibbs-Boltzmann (G-B) weight. This method has already been successfully applied to the ground-state sampling of three-dimensional Ising  $\pm J$  spin glasses<sup>6</sup>. Here, the method is extended to the  $T > 0$  case and again applied to the  $d = 3 \pm J$  SG model. Please note that this approach works better and better with *decreasing* temperature, hence is complementary to the MC technique, which suffers from equilibration problems at low temperatures. But similar to MC, one has to monitor some measured quantities as a function of some parameters to establish equilibration, e.g. the number of clusters found in the analysis as a function of the number of states included. Also similar to MC, obtaining equilibrium becomes harder with increas-

ing system size. In this sense, the method is also not exact. But in contrast to MC, ensuring equilibrium in this way is possible at very low temperatures for larger systems (and becomes impossible for higher temperatures), while for MC it is the other way round.

We apply the algorithm to three-dimensional Ising spin glasses. The EA model consists of  $N = L^3$  Ising spins  $s_i = \pm 1$  on a cubic lattice with the Hamiltonian  $H = -\sum_{\langle i,j \rangle} J_{ij} s_i s_j$ . The sum runs over all pairs of nearest neighbors  $\langle i,j \rangle$ . The  $J_{ij}$  are quenched random variables taking values  $J_{ij} = \pm 1$  with equal probability and satisfy the constraint  $\sum_{\langle i,j \rangle} J_{ij} = 0$ . We apply periodic boundary conditions in all directions.

In this work we show that the overlap distribution  $P(q)$  at zero temperature is qualitatively different from  $P(q)$  at low but non-zero temperature. This means, even if there is an exponential number of GS configurations, zero-temperature quantities may be very different from those at any finite and small temperature. In particular we will show here that for the three-dimensional EA model, which has a finite zero-temperature entropy,  $P(q)$  is very narrow at exactly  $T = 0$ , while it is broad at any finite temperature. We obtained the same result for the box-overlap  $P_{\text{box}}(q)$ . The picture resulting from our findings is that of a large number of GS which are however very close. Nevertheless, quite different states can be easily found once the first excited energy levels are considered. This picture agrees with the very recent MC results by Palassini and Young<sup>7</sup>.

Before proceeding with our results and methods, we show, as a motivation, results from applying the SimA method to one sample realization of site  $L = 5$  of our model. We have performed  $10^4$  independent runs of the SimA algorithm, starting with a temperature  $T_0 = 2$  and reducing the temperature according  $T_{n+1} = bT_n$  until  $T = 0.1$  is reached. Per temperature 10 MC sweeps were performed. At the end of the simulation, one randomly chosen configuration exhibiting the lowest energy encountered during the run was stored. After having performed  $10^4$  runs, only the true ground states were kept. A GS configuration and its mirror image, obtained by reversing all states, are treated as being equivalent. As it turns out, the system has 59 distinct GS configurations. In Fig. 1 histograms of the number of times each GS has been found are displayed for  $b = 0.5$  and  $b = 0.99$ . One sees clearly that for  $b = 0.5$  different GS configurations occur with different frequencies<sup>8</sup>, i.e. not all appear with the same frequency as requested by the G-B distribution. When cooling much slower, i.e. with  $b = 0.99$ , all GS are almost equiprobable. This means that just finding GS configurations is much easier than finding each GS configuration with the correct probability.

For system sizes just slightly larger than  $L = 5$ , the number of GS and excited states is already huge (e.g.  $\sim 10^{16}$  for  $L = 8$ ). For this system sizes it is impossible to obtain a histogram similar to the one presented above. Consequently, it is impossible to determine whether all GS are sampled with the correct statistics.

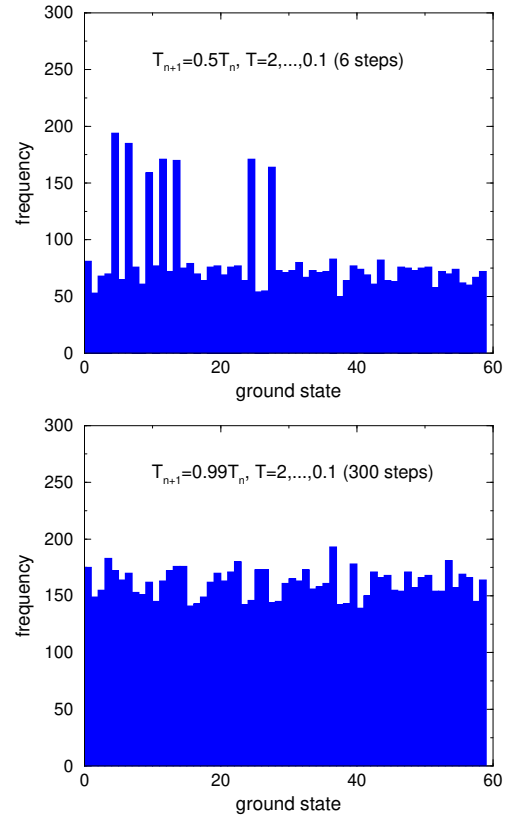


FIG. 1: Histogram of the number of times each GS is found with a SimA simulation of  $10^4$  independent runs for one  $L = 5$  realization of a  $\pm J$  Ising spin glass. The temperature was decreased according to  $T_{n+1} = bT_n$ , with  $T_0 = 2$  until  $T = 0.1$  is reached. At each temperature 10 MC sweeps were performed. For the upper panel  $b = 0.5$ , while  $b = 0.99$  for the lower panel.

This is even more true for excited states. Please note that this is the same for more elaborate algorithms like parallel tempering<sup>9</sup>. Since, as already pointed out, at very low temperatures and for system sizes like  $L = 10$  it is impossible to equilibrate the system, other methods have to be applied. In this paper, we present a post-processing tool, which allows to correct the bias imposed by any algorithm and leads to an equilibrated sample. For sizes up to  $L = 10$  and low temperatures up to  $T < 0.5$  the additional effort is moderate, because only the few lowest levels of excited states have to be considered. For larger temperatures, the post-processing methods becomes intractable, but then conventional MC methods can be easily applied.

The rest of the paper is organized as follows. First, we explain the algorithms we have applied. In the next section, we present the result for the three-dimensional  $\pm J$  spin glass. Finally, a summary and a discussion are given.

## II. ALGORITHMS

The technique to obtain an equilibrated low-temperature sampling consists of four steps:

1. Generate configurations for GS and the lowest levels of excitations.
2. On each energy level: group configurations into clusters.
3. Calculate sizes of clusters.
4. Generate a sample of states for given temperature  $T$ , where each cluster contributes with a weight proportional to its size and to the G-B factor  $\exp(-E/T)$ , where  $E$  is the energy of the configurations in that cluster.

Now all four steps are explained.

The basic method used here to generate the configurations is the cluster-exact approximation (CEA) technique<sup>10</sup>, which is a discrete optimization method<sup>5</sup> designed especially for spin glasses. In combination with a genetic algorithm<sup>11,12</sup> this method is able to calculate true GS<sup>13</sup> up to  $L = 14$ , as well as excited configurations as a byproduct. Since the CEA technique is well established and described in several sources, the details are skipped here. For each system and each energy level, we have generated 1000 configurations with the pure genetic CEA algorithms. We will show below that this number of configurations is sufficient up to  $L = 10$  and  $T = 0.5$ .

By applying pure genetic CEA, one does not obtain the true thermodynamic distribution<sup>14</sup>, i.e. not all configurations with the same energy contribute to physical quantities proportional to the G-B weight. This means the genetic CEA algorithm is biased. For small system sizes up to  $L = 4$  it is possible to avoid the problem by generating *all* low-energy configurations; averages can be performed simply by considering each configuration once, weighted with the G-B factor. Since the degeneracy increases exponentially with the number  $N$  of spins and grows also strongly with the energy level, a complete enumeration is not possible for larger system sizes or higher energies. Instead, one has to choose a subset of all configurations, where each configurations contributes with a probability proportional to the G-B weight. The procedure described here, consisting of steps 2-4 mentioned above, is applied to ensure that all configurations appear with the correct probability in this selection. Please note that the following methods works for any set of states, independently of the method which has been applied to generate the states. I.e. also the results of many independent runs of a low-temperature MC simulation can be treated, in case an equilibration was not possible, e.g. for very low temperatures and larger system sizes.

In step 2 of our method, we group the configurations into *clusters* by performing the ballistic-search algorithm<sup>15</sup>: All configurations which are accessible via flipping of spins having zero local field (called *free spins*

in the following), i.e. without changing the energy  $E$ , are considered to be in the same cluster. Please note that the Hamiltonian is symmetrical with respect to flipping all spins simultaneously. Hence, for the rest of the paper and for all analysis steps, a configuration and its mirror image are regarded as being identical. The final result is a list of different clusters whose sizes are estimated as explained below. This list does not change if more than one configuration was initially found in the same cluster, since these cases are recognized and correctly handled. For completeness and to convince the reader that the method indeed works, we present some details in the following.

The algorithm is applied independently for all configurations having the same energy. The starting point is a set of  $n_S$  configurations. For clarity, first the *straight-forward method* to obtain the cluster structure is explained. This method will *not* be applied finally. Afterward, the method actually used is exposed.

The straight-forward construction starts with one arbitrary configuration. It is the first member of the cluster. All configurations which differ only by the orientation of one free spin are called *neighbors*. All the neighbors of the starting configuration are added to the cluster. These neighbors are treated recursively in the same way: All their neighbors which are yet not included in the cluster are added, etc. After the construction of one cluster is completed the construction of the next one starts with a configuration, which has not been visited so far.

The construction of the clusters needs only linear computer-time as function of  $n_S$  ( $O(n_S)$ ), similar to the Hoshen-Kopelman technique<sup>16</sup>, because each configuration is visited only once. Unfortunately the detection of all neighbors, which has to be performed at the beginning, is of  $O(n_S^2)$  since all pairs of states have to be compared. Even worse, all existing configurations of a given energy must have been calculated before. As e.g. a  $5^3$  system may exhibit already more than  $10^5$  GS and much more excited states, this algorithm is not suitable.

Instead we use the following technique, based on the *ballistic-search* algorithm<sup>15</sup>. The basic idea of ballistic search is to use a *test*, which tells whether two configurations are in the same cluster. The test works as follows: Given two independent replicas  $\{\sigma_i^\alpha\}$  and  $\{\sigma_i^\beta\}$  let  $D$  be the set of spins, which are different in both states:  $D \equiv \{i | \sigma_i^\alpha \neq \sigma_i^\beta\}$ . Now BS tries to build a path of successive flips of free spins, which leads from  $\{\sigma_i^\alpha\}$  to  $\{\sigma_i^\beta\}$  while using only spins from  $D$ . In the simplest version iteratively a free spin is selected randomly from  $D$ , flipped and removed from  $D$ . This test does not guarantee to find a path between two configurations which belong to the same cluster, since it may depend on the order the spins are selected whether a path is found or not. But, if a path is found, then it is sure that both configurations belong to the same cluster. On the other hand, if both configurations belong to the same cluster, then the method finds a path with a certain probability which depends on the size of  $D$ . It turns out that the proba-

bility decreases monotonically with  $|D|$ . For example for  $N = 8^3$  the method finds a path in 90% of all cases if the two states differ by 34 spins. More analysis can be found in<sup>15</sup>.

The algorithm for the identification of clusters utilizes a collective effect, to overcome the problem that sometimes a path is not found, even if two configurations belong to the same cluster. It works as follows: the basic idea is to let a configuration *represent* that part of a cluster which can be found using BS with a high probability by starting at this configuration. If a cluster is large it has to be represented by a collection of states, such that the whole cluster is “covered”. For example a typical cluster of a  $8^3$  spin glass consisting of  $10^{16}$  ground states is usually represented by only some few ground states (e.g. two or three). A detailed analysis of how many representing configurations are needed as a function of cluster and system size can be found in<sup>15</sup>. The details of the algorithm are as follows: in memory a set of clusters consisting each of a set of representing configurations is stored. At the beginning the cluster set is empty. Iteratively all available configurations  $\{\sigma_i\}$  are treated: For all representing configurations the BS algorithm tries to find a path to the current configuration or to its inverse. If no path is found, a new cluster is created, which is represented by the actual configuration treated. If  $\{\sigma_i\}$  is found to be in exactly one cluster nothing special happens. If  $\{\sigma_i\}$  is found to be in more than one cluster, it is called a *bridge configuration* and all these clusters are merged into one single cluster, which is now represented by the union of the states which have represented all clusters affected by the merge. After all configurations have been treated the whole process is run again with the obtained set of clusters. This allows to find bridge configurations which have not identified in the first iteration, because accidentally only one cluster had been created during the first iteration, at the time the configuration was treated<sup>15</sup>.

The BS identification algorithm has some advantages in comparison with the straight-forward method: since each ground-state configuration represents many ground states, the method does not need to compare all pairs of states. Each state is compared only to a few number of representing configurations. Thus, the computer time needed for the calculation grows only a little bit faster than  $O(n_S n_C)$ <sup>15</sup>, where  $n_C$  is the number of clusters, which is much smaller than  $n_S$ . Consequently, large sets of configurations, which appear already for small system sizes like  $N = 5^3$ , can be treated. Furthermore, the cluster structure of even larger systems can be analyzed, since it is sufficient to calculate a small number of configurations per cluster. The main point is that one has to be sure that all clusters are identified correctly. This is not guaranteed immediately, since for two configurations belonging to the same cluster there is just a certain probability that a path of free flipping spins connecting them is found. But this poses no problem, because once at least one state of a cluster has been found, many

more states can be obtained easily by just performing a  $E = \text{const}$  Monte-Carlo simulation starting with the initial state. Hence, one can increasing the number of states available quickly. The probability that all clusters have been identified correctly approaches very quickly unity with increasing number of available states. Detailed tests can be found in<sup>15</sup>. For all results presented here, we have checked that the clusters do not change when doubling the number of states.

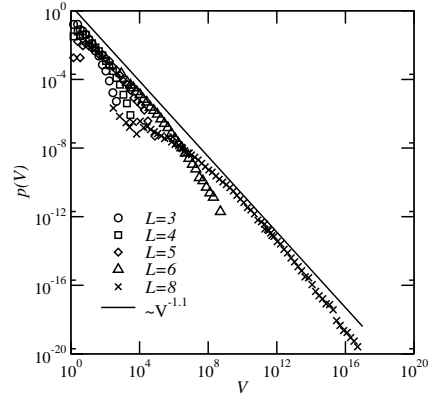


FIG. 2: Cluster-size distributions of GS clusters for small sizes  $L = 3$  to  $L = 8$ . The straight line represents the function  $2V^{-1.1}$ .

Furthermore, one has in principle to ensure that really all clusters are found, which is simply done by calculating enough configurations, but this is still only a tiny fraction of all configurations<sup>15</sup>. This time, the configurations must be obtained independently, one cannot use the  $E = \text{const}$  MC simulation as above. It is possible to obtain at least one configuration from each cluster roughly up to size  $L = 8$  at GS level, resp.  $L = 6$  for first excited states. For sizes like  $N = 10^3$ , the largest size we have treated in this paper, the number of clusters is too large at any energy level. But this is not a problem in principle because the low-temperature behavior of these systems is dominated by large clusters. As an example, in Fig. 2 the probability densities of cluster sizes for GS clusters are shown. The distributions are for small system sizes up to  $L = 8$ , were we can be fairly sure<sup>17</sup> that all clusters have been found<sup>18</sup>. The distributions follow roughly an algebraic decrease with a  $p(V) \sim V^{-\alpha}$  behavior with  $\alpha \sim 1.1$ . This dependence gets straighter with increasing system size. We are interested in the contribution of a cluster of *order* (or scale) of size  $V$  to the behavior. First,

the statistical weight of a cluster is proportional to the number of states in the cluster, i.e. to the volume  $V$ . Second, each scale of cluster sizes contributes proportional to the scale itself, because we are integrating over all clusters of a given scale, i.e. this weight is also proportional to  $V$ . (Or in other words, to translate the probability densities into probabilities on a logarithmic scale, one has to multiply with  $V$ .) In total, clusters of sizes with scale  $V$  contribute with weight  $V^2 p(V) = V^{2-\alpha}$ . Since  $\alpha \approx 1.1 < 2$ , the largest scale clusters dominate the behavior. On the other hand, since  $p(V)$  rapidly decreases, the *number* of these dominating clusters is rather small, i.e. it is rather simple to obtain an equilibrated sample of configurations. For the first excited level we have found  $\alpha = 1.3 < 2$ , while at higher excited levels the number of clusters is too large to really find *all* of them. This results indicates that at higher levels the distribution becomes broader, which limits the application of the method to the lowest level of excitations. This effect is studied below with more detail. We have restricted our analysis to the first 4 levels of excited states.

Please note that the CEA method generates configurations from larger clusters with larger probability<sup>19</sup>, hence the large and important clusters are encountered on average first in the calculations. For the system sizes we have treated here, except  $L = 10$  and  $T = 0.5$ , about 90% of all contributing states are typically from the top 5 largest clusters and further 5% from the next 5 largest clusters. Then with the 1000 configurations we generated per energy level, we encounter typically up to 100 clusters, and we can be pretty sure that all thermodynamic relevant contributions are considered within the level of accuracy given by our statistical fluctuations. Only the results for  $L = 10$  and  $T = 0.5$ , where higher level excitations contribute significantly, may not be equilibrated. This is demonstrated at the end of this section, after we have presented the remaining parts of our algorithm.

The third step in the algorithm is the estimation of the cluster sizes. This works as follows. Let  $\mathcal{C}$  be a cluster we want to measure in size and let's consider a random ‘reference configuration’  $\{r_i\}$  belonging to this cluster. We define a test Hamiltonian  $\tilde{H}[s] = -\sum_i r_i s_i$  for  $\{s_i\} \in \mathcal{C}$ , being  $\tilde{E}(\beta)$  and  $\tilde{S}(\beta)$  the average extensive energy and entropy at inverse temperature  $\beta$ . Then the size of  $\mathcal{C}$  is given by  $\exp[\tilde{S}(0)]$ . Since the GS of this Hamiltonian is unique (it is the reference configuration), i.e.  $\tilde{S}(\infty) = 0$ , we obtain from the microcanonical definition of the temperature  $T = d\tilde{E}/d\tilde{S}$

$$\begin{aligned} \tilde{S}(0) &= \tilde{S}(0) - \tilde{S}(\infty) = \Delta\tilde{S} = \int_{\tilde{E}(\infty)}^{\tilde{E}(0)} \beta d\tilde{E} = \\ &= \int_0^\infty [\tilde{E} - \tilde{E}(\infty)] d\beta = \int_0^\infty (\tilde{E} + N) d\beta \quad , (1) \end{aligned}$$

where the previous last equality comes from an integration by parts and the last equality from the substitution  $\tilde{E}(\infty) = -N$ . In order to calculate this integral, we actually perform a fast MC simulation restricted to

configurations  $\{s_i\} \in \mathcal{C}$  while varying  $w = \exp(-2\beta)$  in  $[0, 1]$  and measuring the average energy  $\tilde{E}$  as a function of  $w$ . The final formula is the integral of a smooth function  $\Delta\tilde{S} = \int_0^1 \frac{N+\tilde{E}}{2w} dw$ . The number of MC sweeps applied per integration step was chosen automatically by the program in a way that the resulting entropy did not change by more than 5% of the value when the number of MC sweeps was doubled. I.e. the program started always with 10 MC sweeps, calculated the entropy integral, then applied 20 MC sweeps and so on. For small clusters, the calculation usually stopped after 20 MC sweeps. For the largest clusters encountered here, the algorithm stopped after the integration using 640 MC sweeps. We have also checked, that for these cases the measured entropy did not depend monotonically on the number of MC sweeps, i.e. we are sure that we did not miss a systematic trend when stopping the calculation at one point.

In principle, there could be high entropic barriers, which prevent the size calculation from converging to the correct value. Fortunately, the full algorithm is not susceptible to that problem. The reason is that the BS clustering method uses single spin flips at constant energy as well to determine the cluster structure, as described above. This means, if two parts of a cluster are connected through a very tiny path (the entropic barrier), which is not detected by the MC integration, the clustering method is also not able to recognize both subclusters as belonging to the same cluster. Hence, if both subclusters are large, the genetic CEA method will have calculated with high probability configurations from both subclusters. In the analysis, because they are not identified as belonging to the same cluster, they will appear as two independent large cluster, i.e. the correct statistics is ensured at the end. If on the other hand, one subcluster is small, it has a negligible contribution to the overall behavior, like other small clusters.

After estimating the cluster sizes, a certain number of configurations is selected from each cluster, this is the last step of the algorithm listed in the beginning of this section. This number of configurations is proportional to the size of the cluster and to the G-B factor  $\exp(-E/T)$ . It means that each cluster contributes with its proper weight. This is possible for small temperatures and small sizes, where only few low-energy levels contribute to the thermodynamical behavior.

The selection of the configurations is done in a manner that many small clusters may contribute as a collection as well<sup>6</sup>. For example, assume that 100 configurations are selected from a cluster consisting of  $10^{10}$  configurations, then for a set of 500 clusters of size  $10^7$  each (with the same energy) a total number of 50 configurations is selected, i.e. 0.1 configurations per cluster on average. The correct handling of such situations is achieved by first sorting all clusters in ascending order. Then the generation of configurations starts with the smallest cluster. For each cluster the number of configurations generated is proportional to its size, to  $\exp(-E/T)$  and to a factor  $f$ . If the number of configurations grows too large,

only a certain fraction  $f_2$  of the configurations which have already been selected is kept, the factor is recalculated ( $f \leftarrow f * f_2$ ) and the process continues with the next cluster.

The configurations representing the clusters are generated from the initial configurations, obtained from the heuristic algorithm, by microcanonical MC simulation, i.e. iteratively spins are randomly selected and flipped if they are free. Since within a cluster there are no energy barriers, for the system sizes up to  $L = 10$ , applying 100 MC sweeps ensures that all configurations within a cluster are visited with the same frequency.

To summarize, by applying the algorithm presented here, each cluster appears with a weight proportional to its size and to  $\exp(-E/T)$  and each configuration within a cluster appears with the same probability. Therefore, on total, the correct thermodynamic distribution is obtained.

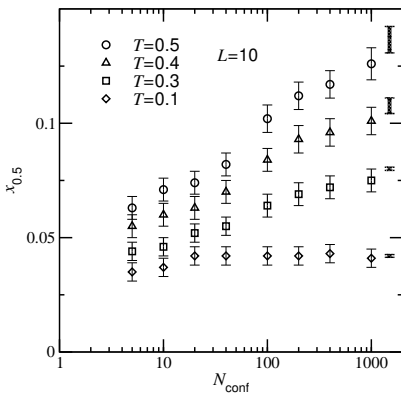


FIG. 3: Result for  $x_{0.5}$  (see Eq. (2) for definition) as a function of the number  $N_{\text{conf}}$  of configurations included per energy level in the analysis. The error bars at the right represent the limiting values  $N_{\text{conf}} \rightarrow \infty$  obtained from fitting the data points  $N_{\text{conf}} \geq 40$  to algebraic functions. For small temperatures  $T$ , few configurations are sufficient while at  $T = 0.5$  more than 1000 configurations are necessary.

We have tested whether our generated data represents the equilibrium behavior by calculating the small-overlap weight  $x_{0.5}$ , as defined in the beginning of the next section in Eq. (2).  $x_{0.5}$  is obtained for the largest system size  $L = 10$  and for different temperatures  $T$  as a function of the number of configurations  $N_{\text{conf}}$  included in the analysis per energy level. The result is shown in Fig. 3. Please note that the full analysis, as explained in this section, has to be repeated independently for each number

$N_{\text{conf}}$ . The configurations were taken in the order they appeared in the generation using the genetic CEA, i.e. for a small number of configurations, the large clusters are more likely to be represented than the smaller clusters since genetic CEA preferentially generates configurations from larger clusters. One can see that for low temperatures, even few generated configurations are sufficient to yield the true behavior. Please note that the remaining fluctuations are due to the fluctuations between the different samples of configurations. The reason that few configurations are sufficient here is that at low temperatures the GSs dominate and the number of GS clusters is fairly small. With increasing temperature, excited states become more important. For excited states, much more clusters exists. Thus, more configurations must be included into the analysis. This is visible in Fig. 3, where at e.g.  $T = 0.5$   $x_{0.5}$  depends strongly on  $N_{\text{conf}}$ . For  $N_{\text{conf}} = 1000$   $T = 0.5$  seems to be the borderline case, while for  $T < 0.5$  the result for  $x_{0.5}$  seems to be converged (within error bars). We have checked this explicitly by fitting algebraic functions to the data points  $N_{\text{conf}} \geq 40$ , resulting in an agreement within error bars of the limiting value  $N_{\text{conf}} \rightarrow \infty$  with the result we have obtained at  $N_{\text{conf}} \rightarrow \infty$ . Hence we can be again confident that using 1000 configurations per energy level, the results obtained here up to  $L = 10$  and  $T < 0.5$  represent the true equilibrium behavior or, at least, is so close to the true result that it cannot be distinguished from it at the level of accuracy determined by the statistical fluctuations. For smaller sizes, the number of clusters is smaller on each energy level, which means that 1000 configurations per realization and energy level are sufficient for even higher temperatures. But we restrict our analysis to  $T \leq 0.5$  here.

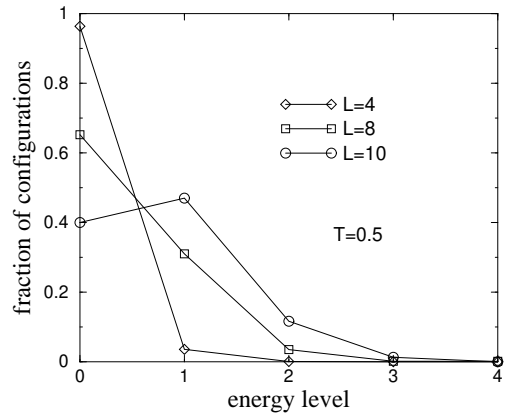


FIG. 4: Fraction of configurations sampled from each energy level at  $T = 0.5$  for different system sizes. Energy level 0 is the ground state. Lines are guides to the eyes only.

Finally, in Fig. 4, the fraction of configurations sampled at  $T = 0.5$  for the different energy levels is shown for different system sizes. For the smallest size  $L = 4$  almost

only GS configurations contribute to the thermodynamics, while increasing system size higher energy configurations become more important. Please note that only for  $L = 10$  configurations from excitation level 3 contribute. There the degeneracy is much larger than for the lower levels. This explains, why the result for  $L = 10$  and  $T = 0.5$  is probably not equilibrated. The result of Fig. 4 shows that, when studying the low-temperature behavior of glassy systems, it is not sufficient to study just GS configurations since the G-B factor and the size of the cluster (i.e. the entropy) must be taken into account. Nevertheless for low temperatures and not too large system sizes, the energy levels which actually contribute to the partition function are very few.

### III. RESULTS

We have calculated ground states and excited configurations up to level four, for system sizes  $L \leq 10$ . Up to 3000 realizations of the disorder were considered (900 for the largest system size). From the set of configurations, samples of several hundred equilibrium configurations were generated for temperatures  $T \in [0, 0.5]$ .

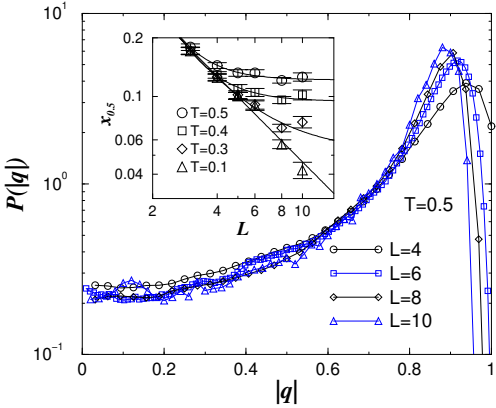


FIG. 5: Distribution  $P(|q|)$  of overlaps at  $T = 0.5$  for different system sizes. Lines are guides to the eyes only. The inset shows the average weight  $x_{0.5}$  of the distribution for  $|q| \leq 0.5$  as a function of system size for  $T = 0.5, 0.4, 0.3, 0.1$ . The lines represent fits to functions of the form  $x(L) = x^\infty + a L^\lambda$ , with  $x^\infty \equiv 0$  and  $\lambda = -1.10(5)$  for  $T = 0.1$ ,  $x^\infty = 0.051(13)$  for  $T = 0.3$ ,  $x^\infty = 0.095(4)$  for  $T = 0.4$  and  $x^\infty = 0.122(4)$  for  $T = 0.5$ .

For each disorder realization and each temperature, the distribution  $P_J(q)$  of overlaps  $q \equiv \frac{1}{N} \sum_i s_i^\alpha s_i^\beta$  was calculated, where  $\{s_i^\alpha\}$ ,  $\{s_i^\beta\}$  are two different equilibrium configurations. In Fig. 5 the disorder-averaged distribution  $P(|q|) = [P_J(|q|)]_J$  is shown for  $T = 0.5$ , where  $[\dots]_J$  denotes the average over the quenched disorder. The long tail to  $q = 0$  seems to saturate at a finite weight, indicating the existence of a complex low-energy landscape

at finite temperatures. This can be seen even better, by calculating the fraction

$$x_{q_0} = \int_{-q_0}^{q_0} P(q) dq \quad (2)$$

of overlaps smaller than  $q_0$ . The result for  $q_0 = 0.5$  is presented in the inset of Fig. 5. For zero temperatures, where only GS configurations are sampled,  $x_{0.5}$  converges to 0 or to a very small value<sup>20</sup>. The rate of convergence is described by the finite-size dependence  $x_{0.5}(L) \sim L^\lambda$ . We find  $\lambda = -1.10(5)$ , which is compatible with the predicted bound  $\lambda \leq -1$  given by the “TNT”-scenario<sup>21</sup>. In Ref. 7 a larger value  $\lambda = -0.90(10)$  was found. This slight difference might be due to the different ensembles studied, since in Ref. 7 the constraint  $\sum_{\langle i,j \rangle} J_{ij} = 0$  was not applied.

Please note that for small temperatures we sample only GS configurations, due to small system sizes. For larger temperatures  $T \geq 0.3$ , the asymptotic value of  $x_{0.5}$  is clearly larger than zero. Please note that the last point  $L = 10, T = 0.5$  may not be converged, as discussed above. But, as you can see in Fig. 3, the value of  $x_{0.5}$  is an *increasing* function of the number of states included in the calculation. Hence, the true result (we have obtained  $x_{0.5}^{L=10}(0.5) = 0.137(6)$  as opposed to 0.126(7) found for  $N_{\text{conf}} = 1000$ ) **FEDE: the sentence in parenthesis is not clear! Is 0.137(6) the limit for  $N_{\text{conf}} \rightarrow \infty$ ?** is probably above our value, thus supporting even more the conclusion that  $x_{0.5} > 0$ .

Our results are quantitatively comparable to the data found in Ref. 7 which were obtained by a parallel-tempering MC simulation. Although the authors had no reliable criterion to check equilibration of the system (in contrast to the case with Gaussian distribution of the disorder<sup>3</sup>), by comparison with our results it is very likely that in Ref. 7 indeed thermal equilibrium was obtained.

A non-trivial distribution of overlaps is not a sufficient criterion for a complex energy landscape. A qualitatively similar overlap distribution with a nonzero weight for small values of  $q$  would be obtained also for a system, where various configurations differ by a domain wall through the system at different positions, e.g. a ferromagnet with antiperiodic boundary conditions in one direction<sup>22</sup>.

To rule out this scenario, we have calculated also the distributions of box (or window) overlaps<sup>23,24</sup>. This overlap is defined as usual, but restricted to a finite “window” of volume  $l \times l \times l$ , with  $l < L$  fixed independently of the system size  $L$ . Please note that for the aforementioned ferromagnet, the distribution of box overlaps converges to a pair of delta functions at  $q = \pm 1$  when  $L \rightarrow \infty$ . The result for  $l = 3$ ,  $T = 0.5$  is exhibited in Fig. 6. At finite temperature, similar to the conventional overlap, the low- $q$  tails seems to saturate, but more slowly, at a non-zero weight with increasing systems size. This can be seen from the inset of Fig. 6, where  $x_{0.5}$  is shown as a function of system size for  $T = 0.1, 0.3, 0.4$  and  $T = 0.5$ . For  $T \geq 0.3$ ,  $x_{0.5}$  clearly converges to a nonzero value.

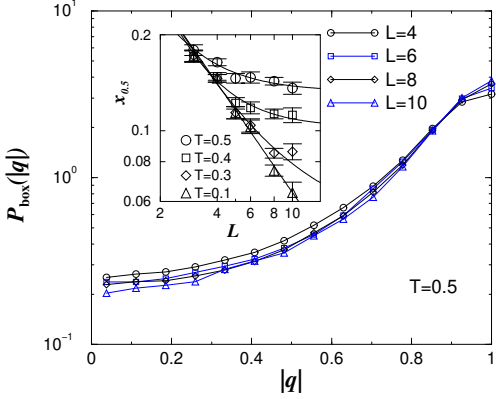


FIG. 6: Distribution  $P_{\text{box}}(|q|)$  of box overlaps at  $T = 0.5$  for different system sizes. Lines are guides to the eyes only. The inset shows the average weight  $x_{0.5}$  of the distribution for  $|q| \leq 0.5$  as a function of system size for  $T = 0.5, 0.4, 0.3, 0.1$ . The lines represent fits to functions of the form  $x(L) = x_{\text{box}}^{\infty} + a_b L^{\lambda_b}$ , with  $x_{\text{box}}^{\infty} \equiv 0$  and  $\lambda_b = -0.86(5)$  for  $T = 0.1$ ,  $x_{\text{box}}^{\infty} = 0.05(13)$  for  $T = 0.3$ ,  $x_{\text{box}}^{\infty} = 0.10(1)$  for  $T = 0.4$  and  $x_{\text{box}}^{\infty} = 0.13(1)$  for  $T = 0.5$ .

Thus, we can conclude that indeed at finite temperatures, three-dimensional spin glasses exhibit a complex low-energy landscape.

Please note that the non-trivial behavior occurs for low temperatures, probably for all temperatures  $T > 0$ , which are sufficiently far away from the phase transition  $T_c \approx 1.1$ . Hence, the effects which were found within a Migdal-Kadanoff approximation scheme<sup>25</sup> are unlikely to explain the kind of behavior we find.

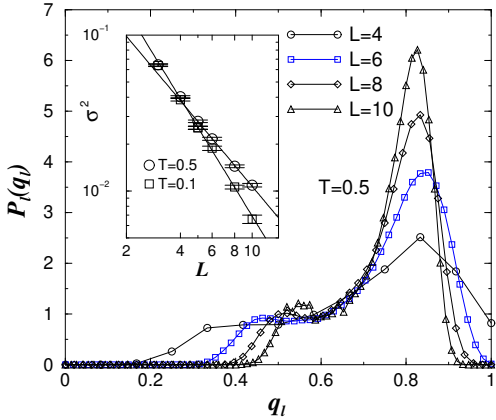


FIG. 7: Distribution  $P_l(q_l)$  of link overlaps at  $T = 0.5$  for different system sizes  $L$ . Lines are guides to the eyes only. The inset shows the variance  $\sigma^2$  as a function of system size  $L$  for  $T = 0.1, 0.5$ . The lines represent fits to functions of the form  $\sigma^2(L) = a_l L^{\lambda_l}$  ( $L > 4$ ), with  $\lambda_l = 0.53(5)$  for  $T = 0.1$  and  $\lambda_l = 0.27(1)$  for  $T = 0.5$ .

Finally, we have computed the average distribution

$P_l(q_l)$  of link overlaps  $q_l \equiv \sum_{\langle i,j \rangle} s_i^{\alpha} s_j^{\alpha} s_i^{\beta} s_j^{\beta}$ . The result for  $T = 0.5$  and different system sizes can be observed in Fig. 7. The distribution becomes narrower, but a second small peak seems to emerge. In the inset of Fig. 7 the finite-size dependence of the variance  $\sigma^2 = \int_0^1 (q - \bar{q})^2 P_l(q) dq$  is shown for different temperatures. In all cases, the width seems to converge toward zero. Please note, however, that we cannot exclude that the variance converges to a small but finite value. When we fit it to a function of the form  $\sigma^2(L) = \sigma_{\infty}^2 + a_{\sigma} L^{\lambda_{\sigma}}$  we obtain, for  $T = 0.5$ ,  $\sigma_{\infty}^2 = 0.0038(28)$  with  $\chi^2$  per degree of freedom of 0.1, which is a very good fit. Nevertheless, a  $P_l(q_l)$  consisting of two peaks at distance of 0.1 with weights 0.1 and 0.9 respectively has a variance  $\sigma^2 = 0.0009$ .

The behavior of  $P_l(q_l)$  is quantitatively the same for three-dimensional spin glasses with a Gaussian distribution of the interactions<sup>3</sup>, which were found with a parallel-tempering MC simulation.

#### IV. SUMMARY

Summarizing, we have presented an algorithm which allows to investigate the low-temperature behavior of Ising systems with high degeneracy by direct sampling of GS and excited configurations. The basic idea is to generate configurations with any suitable algorithm, group the configurations into clusters, measure the size of the clusters and then obtain a very good estimate of the G-B measure, to sample configurations with. Similar to MC, where one has to increase the number of MC sweeps until the system is equilibrated, one has to increase the number of independent configurations until the true behavior is obtained. The main difference to MC techniques is that the method presented here works better with decreasing temperature, while MC equilibrates faster with increasing temperatures. In this sense these methods are complementary.

We have applied the algorithm to study the low-temperature behavior of three-dimensional  $\pm J$  Ising spin glasses. We find that the statistical properties of the exponentially many ground state configurations are not representative of the low-temperature behavior. In particular we have shown for the three-dimensional Edwards-Anderson model that both the distributions of the overlap and of the box-overlap seem to be very narrow functions at  $T = 0$ , where only few states contribute to the G-B measure, and broad for finite  $T$ . Hence the model does have a complex state space, which seems to become trivial at  $T = 0$ . For this reason one is forced to probe the energy landscape at  $T > 0$ . The distribution of the link-overlap seems to develop a second peak, but the extrapolation of the asymptotic shape is beyond our present computational capabilities.

## Acknowledgments

The work was supported by the the *Interdisziplinäres Zentrum für Wissenschaftliches Rechnen* in Heidelberg

and the *Paderborn Center for Parallel Computing* by the allocation of computer time. AKH acknowledges financial support from the DFG (Deutsche Forschungsgemeinschaft) under grants Ha 3169/1-1 and Zi 209/6-1.

---

<sup>\*</sup> Electronic address: hartmann@theorie.physik.uni-goettingen.de

<sup>†</sup> Electronic address: Federico.Ricci@roma1.infn.it

<sup>1</sup> For reviews on spin glasses cf.: K. Binder and A.P. Young, Rev. Mod. Phys. **58**, 801 (1986); M. Mezard, G. Parisi, M.A. Virasoro, *Spin glass theory and beyond*, World Scientific, Singapur 1987; K.H. Fisher and J.A. Hertz, *Spin Glasses*, Cambridge University Press, 1991; A.P. Young, *Spin Glasses and Random Fields*, World Scientific, 1998

<sup>2</sup> D.P. Landau and K. Binder, *A Guide to Monte Carlo Simulations in Statistical Physics*, (Cambridge University Press, Cambridge 2000).

<sup>3</sup> H.G. Katzgraber, M. Palassini and A.P. Young, Phys. Rev. B **63**, 184422 (2001).

<sup>4</sup> F. Krzakala and O.C. Martin, Phys. Rev. Lett. **85**, 3013 (2000). M. Palassini and A.P. Young, Phys. Rev. Lett. **85**, 3017 (2000). E. Marinari and G. Parisi, Phys. Rev. B **62**, 11677 (2000); Phys. Rev. Lett. **86**, 3887 (2001).

<sup>5</sup> For an overview see: A.K. Hartmann and H. Rieger, *Optimization Algorithms in Physics*, (Wiley-VCH, Berlin 2001).

<sup>6</sup> A.K. Hartmann, Eur. Phys. J. B **13**, 539 (2000).

<sup>7</sup> M. Palassini and A.P. Young, Phys. Rev. B **63**, 140408(R) (2001).

<sup>8</sup> A further analysis<sup>15</sup> shows that the GS of this system are organized in two clusters, where the GS of each cluster are connected by zero-energy flips of single spins. The GS found more often belong to one cluster, the other GS to the second cluster.

<sup>9</sup> J.J. Moreno, H.G. Katzgraber, and A.K. Hartmann, accepted for publication in Int. J. Mod. Phys. C, preprint cond-mat/0209248

<sup>10</sup> A.K. Hartmann, Physica A, **224**, 480 (1996).

<sup>11</sup> K.F. Pál, Physica A **223**, 283 (1996).

<sup>12</sup> Z. Michalewicz, *Genetic Algorithms + Data Structures = Evolution Programs*, Springer, Berlin 1992

<sup>13</sup> A.K. Hartmann, Phys. Rev. E **59**, 84 (1999)

<sup>14</sup> A. Sandvik, Europhys. Lett. **45**, 745 (1999); A.K. Hartmann, Europhys. Lett. **45**, 747 (1999)

<sup>15</sup> A.K. Hartmann, J. Phys. A **33**, 657 (2000).

<sup>16</sup> J. Hoshen and R. Kopelman, Phys. Rev. B **14**, 3438 (1976)

<sup>17</sup> A.K. Hartmann, Eur. Phys. J. B **8**, 619 (1999); Phys. Rev. E **59**, 84 (1999); Phys. Rev. E **60**, 5135 (1999)

<sup>18</sup> On average, systems of size  $L = 8$  have 24.2 GS clusters. I.e. it is not difficult to be sure that all clusters have been found.

<sup>19</sup> A.K. Hartmann, Physica A **275**, 1 (1999).

<sup>20</sup> G. Hed, A. K. Hartmann and E. Domany, Europhys. Lett. **55**, 112 (2001).

<sup>21</sup> F. Krzakala and O.C. Martin, Europhys. Lett. **53**, 749 (2001)

<sup>22</sup> D.A. Huse and D.S. Fisher, J. Phys. A **20**, L997 (1987)

<sup>23</sup> C.M. Newman and D.L. Stein, Phys. Rev. E **57**, 1356 (1998).

<sup>24</sup> E. Marinari, G. Parisi, F. Ricci-Tersenghi, and J.J. Ruiz-Lorenzo, J. Phys. A **31** L481, (1998).

<sup>25</sup> M.A. Moore, H. Bokil, and B. Drossel, Phys. Rev. Lett. **81**, 4252 (1998); B. Drossel, H. Bokil, M.A. Moore, and A.J. Bray, Eur. Phys. J. B **13**, 369 (2000).